Check for updates

Phosphoproteomics of *Aspergillus fumigatus* Exposed to the Antifungal Drug Caspofungin

Eliciane Cevolani Mattos,[a] Giuseppe Palmisano,[b] Gustavo H. Goldman[a]

[a]Faculdade de Ciências Farmacêuticas de Ribeirão Preto, Universidade de São Paulo, Ribeirão Preto, Brazil
[b]Departamento de Parasitologia, Instituto de Ciências Biomédicas, Universidade de São Paulo, São Paulo, Brazil

ABSTRACT *Aspergillus fumigatus* is an opportunistic and allergenic pathogenic fungus, responsible for fungal infections in humans. *A. fumigatus* infections are usually treated with polyenes, azoles, or echinocandins. Echinocandins, such as caspofungin, can inhibit the biosynthesis of the β-1,3-glucan polysaccharide, affecting the integrity of the cell wall and leading to fungal death. In some *A. fumigatus* strains, caspofungin treatment at high concentrations induces an increase of fungal growth, a phenomenon called the caspofungin paradoxical effect (CPE). Here, we analyze the proteome and phosphoproteome of the *A. fumigatus* wild-type strain and of mitogen-activated protein kinase (MAPK) *mpkA* and *sakA* null mutant strains during CPE (2 μg/ml caspofungin for 1 h). The wild-type proteome showed 75 proteins and 814 phosphopeptides (corresponding to 520 proteins) altered in abundance in response to caspofungin treatment. The $\Delta mpkA$ ($\Delta mpkA$ caspofungin/wild-type caspofungin) and $\Delta sakA$ ($\Delta sakA$ caspofungin/wild-type caspofungin) strains displayed 626 proteins and 1,236 phosphopeptides (corresponding to 703 proteins) and 101 proteins and 1,217 phosphopeptides (corresponding to 645 proteins), respectively, altered in abundance. Functional characterization of the phosphopeptides from the wild-type strain exposed to caspofungin showed enrichment for transcription factors, protein kinases, and cytoskeleton proteins. Proteomic analysis of the $\Delta mpkA$ and $\Delta sakA$ mutants indicated that control of proteins involved in metabolism, such as in production of secondary metabolites, was highly represented in both mutants. Results of functional categorization of phosphopeptides from both mutants were very similar and showed a high number of proteins with decreased phosphorylation of proteins involved in transcriptional control, DNA/RNA binding, cell cycle control, and DNA processing. This report reveals novel transcription factors involved in caspofungin tolerance.

IMPORTANCE *Aspergillus fumigatus* is an opportunistic human-pathogenic fungus causing allergic reactions or systemic infections, such as invasive pulmonary aspergillosis in immunocompromised patients. Caspofungin is an echinocandin that impacts the construction of the fungal cell wall by inhibiting the biosynthesis of the β-1,3-glucan polysaccharide. Caspofungin is a fungistatic drug and is recommended as a second-line therapy for treatment of aspergillosis. Treatment at high concentrations induces an increase of fungal growth, a phenomenon called the caspofungin paradoxical effect (CPE). Collaboration between the mitogen-activated protein kinases (MAPK) of the cell wall integrity (MapkA) and high-osmolarity glycerol (SakA) pathways is essential for CPE. Here, we investigate the global proteome and phosphoproteome of *A. fumigatus* wild-type, $\Delta mpkA$, and $\Delta sakA$ strains upon CPE. This study showed intense cross talk between the two MAPKs for the CPE and identified novel protein kinases and transcription factors possibly important for CPE. Increased understanding of how the modulation of protein phosphorylation may affect the fungal growth in the presence of caspofungin represents an important step in the development of new strategies and methods to combat the fungus inside the host.

Address correspondence to Gustavo H. Goldman, ggoldman@usp.br.

Caspofungin treatment at high concentrations induces an increase of fungal growth, a phenomenon called Caspofungin Paradoxical Effect. We investigate the global proteome and phosphoproteome of the A. fumigatus wild-type, ΔmpkA, and ΔsakA strains upon CPE. @FungalSao

*A*spergillus fumigatus is an opportunistic and allergenic pathogenic fungus that is responsible for a high incidence of fungal infections in humans and several pathologies in immunocompromised individuals. Fungal infections, such as invasive aspergillosis (IA), are usually treated with polyenes, azoles, or echinocandins (1). Polyenes are fungicidal and act by disruption of the fungal cell membrane by physically binding to the membrane ergosterol, resulting in pore formation and cell death (1). Azoles affect the biosynthesis of ergosterol, causing damage to the fungal membrane and resulting in cell death by membrane lysis or inhibition of fungal growth (1). Echinocandins can inhibit the biosynthesis of the β-1,3-glucan polysaccharide, the major component of the fungal cell wall, affecting the integrity of the cell wall and leading to fungal death (1, 2). Triazoles (voriconazole, for example) have fungistatic activities and are applied as a primary treatment in invasive aspergillosis therapy, whereas echinocandins (such as caspofungin [caspo], anidulafungin, and micafungin) act as fungistatic agents and are used as a second-line drug treatment in patients with infections that are recalcitrant to the primary treatments (1–3). The emergence of *A. fumigatus* clinical isolates resistant to azoles and echinocandins has been considered a potential public health issue (4).

In some *A. fumigatus* strains, tolerance to caspofungin at high concentrations induces an increase in fungal growth, a phenomenon called the caspofungin paradoxical effect (CPE) (5, 6). Compensatory reactions such as the transcriptional stimulation of genes encoding chitin synthases and the subsequent increase of chitin content in the cell wall are due to the activation of stress-activated signaling pathways (4, 6). High caspofungin concentrations elicit a spike in cytosolic calcium, which activates calcineurin and CrzA to promote the CPE (7, 8). Upon promotion of the CPE, calcineurin dephosphorylates the transcription factor (TF) CrzA, which is translocated to the nucleus and activates the expression of chitin synthases (9). A novel basic leucine zipper ZipD transcription factor was identified to function in the calcium-calcineurin pathway and was involved in the CPE (9). Recently, we identified four transcription factors whose null mutants are susceptible to calcium and are also involved in CPE (10).

CPE is also dependent on all four *A. fumigatus* mitogen-activated protein kinases (MAPKs). The cell wall integrity (CWI) pathway involving the MAPK MpkA (2) activates the RlmA transcription factor, which regulates the expression of chitin synthase genes in response to different concentrations of caspofungin (9, 11, 12). *A. fumigatus* MAPKs, including high-osmolarity glycerol (HOG) MAPK SakA and MpkC, are also involved in CPE, activating TFs AtfA to AtfD, which are important for CPE maintenance (13, 14). The null mutant for the MAPK MpkB, homologous to yeast Fus3 (15), is more susceptible to caspofungin and had also lost the CPE (15). A cross talk interaction between SakA and MpkA has already been observed for the adaptation to caspofungin (13, 16, 17).

It has been demonstrated that *A. fumigatus* paradoxically growing hyphae emerging from microcolonies are initially devoid of β-1,3-glucan (18) but, intriguingly, that these hyphae expose β-1,3-glucan in later growth stages (18). Fks1 glucan synthase, the main target of caspofungin, relocates to the hyphal tips during these later growth stages, suggesting that β-1,3-glucan synthase activity is restored (18, 19). Interestingly, a novel mechanism has been proposed to explain this increased glucan accumulation and Fks1 relocation to the hyphal tips (20). Analysis of the lipid microenvironment of an Fks1 from an *A. fumigatus* caspofungin-resistant mutant showed an increase in the abundance of dihydrosphingosine (DhSph) and phytosphingosine (PhSph), suggesting that caspofungin induced an alteration in the composition of plasma membrane lipids surrounding Fks1 glucan synthase, rendering it resistant to echinocandins (20).

Genetic or chemical inhibition of heat shock protein 90 (Hsp90) abolished the CPE (21). Besides Hsp90, another molecular chaperone, Hsp70, is also important for the regulation of CPE together with their cochaperone Hop/StiA (22). Transcriptional

A.

| WT response to 2 µg / mL Caspofungin for 1 h	Proteome	Phosphoproteome
Number of total protein/phosphopeptide	3193	9613
Total protein/phosphopeptide p<0.05	75	814 (520)
Protein/phosphopeptide only in WT 0 (total dephosphorylation)	0	153
Protein/phosphopeptide only in WT 2 (total phosphorylation)	5	53
Protein/phosphopeptide present in both with increase of intensity	65	79
Protein/phosphopeptide present in both with decrease of intensity	5	529
Common proteins between proteome and phosphoproteome	5	5

B. **C.** **D.** **E.**
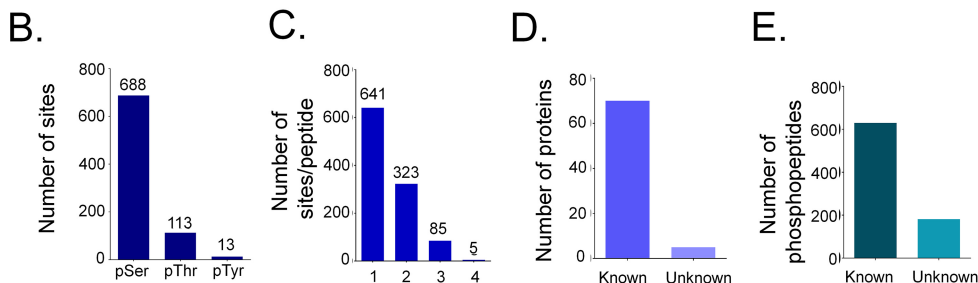
FIG 1 Proteome and phosphoproteome of *A. fumigatus* wild-type strain exposed to caspofungin. (A) Summary table of all proteins and phosphopeptides modulated in wild-type strain upon exposure to caspofungin. (B) Number of phosphorylated residues of serine, threonine, or tyrosine identified. (C) Number of sites of phosphorylation per peptide. (D) Number of proteins. (E) Number of known and unknown proteins.

profiling has shown that the main effect of reducing the Hsp90 effect is the reduction of expression of the genes of the mitochondrial respiratory chain, in particular, that of the genes encoding NADH-ubiquinone oxidoreductases (complex I) (23, 24).

The members of our laboratory are interested in understanding which genetic determinants are involved in *A. fumigatus* CPE. Recently, we evaluated the global *A. fumigatus* phosphoproteome-exposed cell wall damage mediated by Congo red (CR), identifying 485 proteins putatively involved in the cell wall stress response (25). Among these proteins, we have isolated five novel transcription factors (TFs) that were phosphorylated upon exposure to CR. The TF null mutants for three of these genes were more susceptible to CR, calcofluor white (CFW), and caspofungin with reduced CPE (25). Here, we extended these studies by analyzing the proteome and phosphoproteome of the *A. fumigatus* wild-type (WT) and Δ*mpkA* and Δ*sakA* mutant strains during the stress with caspofungin.

RESULTS

Proteome and phosphoproteome analysis of *A. fumigatus* upon caspofungin stress. The study of proteins and their posttranslational modifications in an organism under some stress conditions provided an important insight into the biological processes and signaling pathways modulated during the environmental response. Previously, we had observed that fungal mycelia grown in liquid cultures are more susceptible to high concentrations of caspofungin, and in agreement, the CPE of *A. fumigatus* strain CEA17 was already observed at 2 µg/ml caspofungin in liquid minimal medium (MM) for 1 h, whereas the onset of the CPE was observed at 8 µg/ml on solid medium (9). To understand how *A. fumigatus* reacts to CPE concentrations and about the involvement of MAPKs in that response, we perform proteomic and phosphoproteomic analysis of the wild-type, Δ*sakA*, and Δ*mpkA* strains left untreated (control) or treated with 2 µg/ml caspofungin for 1 h.

To understand the signaling pathways and identify new targets that may be involved in the fungal response to caspofungin, we started our study by the analysis of the wild-type response to the drug. The analysis of total proteins identified 3,193 unique proteins. The wild-type proteome showed that 75 proteins were altered in abundance in response to 2 µg/ml caspofungin treatment, with most of them showing increased total levels (70 proteins with increased versus 5 proteins with decreased total levels) (Fig. 1A; see also Table S1A at https://doi.org/10.6084/m9.figshare.12315212).

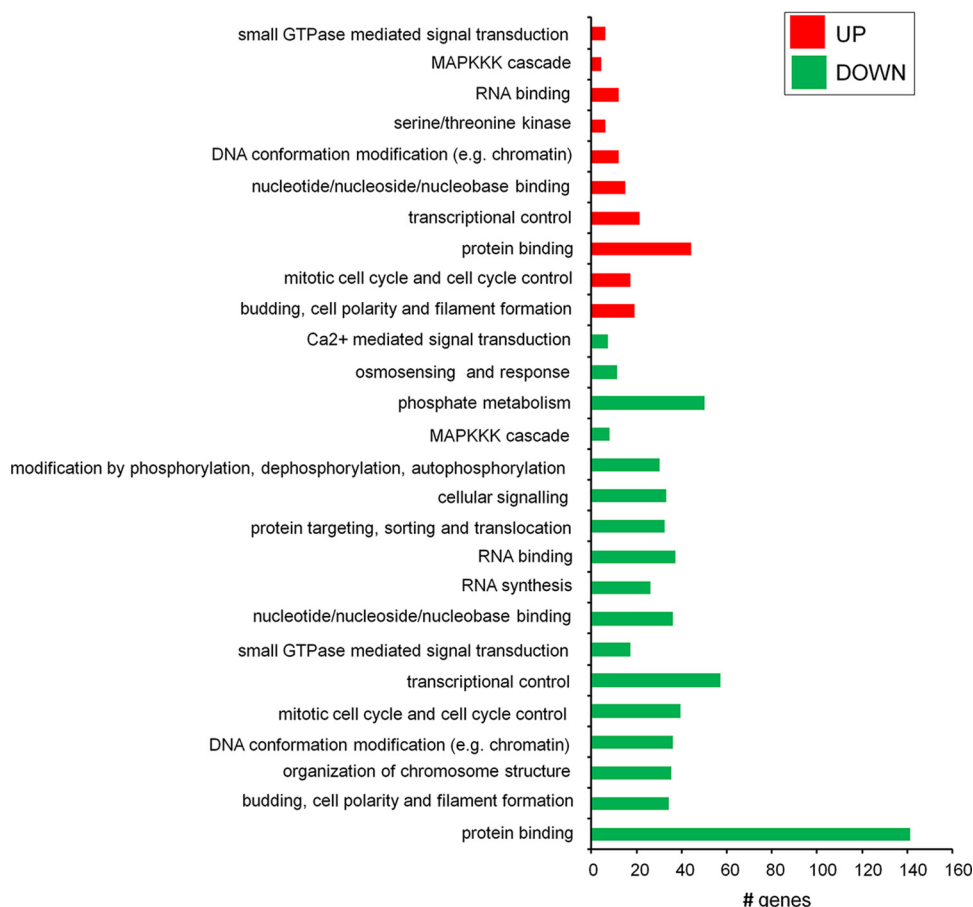## Phosphoproteome Wild-type caspofungin 2 µg/ml / wild-type control

FIG 2 Functional categorization of phosphopeptides differentially phosphorylated in *A. fumigatus* wild-type strain exposed to 2 µg/ml caspofungin treatment for 1 h ($P < 0.05$). The functional enrichment was performed with FungiFun (https://sbi.hki-jena.de/fungifun/fungifun.php), using *A. fumigatus* Af293 as the organism and FunCat as the ontology classification.

The results obtained from samples enriched with TiO_2 enrichment for phosphorylated proteins showed a total of 9,613 phosphopeptides, with 6,522 with localization probability levels higher than 75% (class I phosphosites) (Fig. 1A; see also Table S1B). As determined using Student's *t* test, 814 phosphopeptides were differentially expressed between caspofungin-treated wild-type strain and the control (nontreated [0]), with most of them (682 [83.7%]) being dephosphorylated or decreasing their phosphorylation levels (Fig. 1A; see also Table S1B). The analysis of the sites of phosphorylation indicated the presence of 688 residues of serine, 113 residues of threonine, and 13 residues of tyrosine (Fig. 1B) and indicated 1 (641) or 2 (323) phosphosites per peptide (Fig. 1C).

A functional categorization was performed for proteins and phosphopeptides modulated in the wild-type strain during the drug response. Most of the proteins were found to have unknown functions, but four of them were identified as related to the deoxyribonucleotide metabolism (Fig. 1D). A total of 6,030 phosphopeptides modulated in the wild-type response have known function (Fig. 1E). Results of functional categorization of those phosphopeptides are shown in Fig. 2. Functional characterization of proteins that were downregulated and upregulated with respect to phosphorylation in the presence of caspofungin showed high complexity (Fig. 2). Enrichment was seen for proteins that were downregulated and upregulated with respect to phosphorylation and involved in small-GTPase-mediated signal transduction; the MAPK kinase

kinase kinase (MAPKKK) cascade; the mitotic cell cycle; cell cycle control, cell budding, and cell polarity; filament formation; and transcriptional control (Fig. 2). Interestingly, MAPKKK cascade proteins such as BckA[Bck1], SskB[Ssk2], SteC[Ste11], MpkA[Slt2], and SakA[Hog1] and the MAP phosphatase PtcG (26) were found to be downregulated or upregulated or both (see Table S1 at https://doi.org/10.6084/m9.figshare.12315212).

Analysis of the ΔmpkA and ΔsakA proteome under the control of the fungal response to caspofungin stress. There is an involvement of MAPKs in the response to caspofungin and the modulation of the CPE (13, 15–17, 27, 28). The study of the global profile of protein levels and of protein phosphorylation in strains deleted for those kinases may provide the identification of new targets related to MAPK signaling pathways and drug responses. Results of a total comparison between proteome and phosphoproteome data from the wild-type (WT caspo/control), ΔsakA (ΔsakA caspo/WT caspo), and ΔmpkA (ΔmpkA caspo/WT caspo) strains are shown in Fig. 3A (see also Tables S2 and S3 at https://doi.org/10.6084/m9.figshare.12315212). The ΔmpkA strain was found to have the most distinct proteome profile, with a high number of unique proteins modulated, in comparison with WT and ΔsakA strains (Fig. 3A).

The results of proteomic study of the ΔsakA mutant strain showed that 11 proteins were not present in ΔsakA samples (i.e., were exclusively produced by the WT strains under the same treatment conditions), that 72 proteins had decreased intensity in mutant samples, and that 18 proteins had increased total levels (Fig. 3A and B; see also Table S3A at https://doi.org/10.6084/m9.figshare.12315212). As shown by ΔmpkA proteomic data representing results from treatment with caspofungin at 2 μg/ml, 5 proteins were exclusively produced by the WT samples, and 227 proteins showed a decrease of total level in the mutant strain. Most of the proteins (334) showed increased levels, and 60 proteins were present only in the mutant strain (not found in WT samples) (Fig. 3A and B; see also Table S3A).

In the proteome analysis of the ΔmpkA mutant strain, the functional enrichment data showed upregulation of proteins involved in electron transport and membrane-associated energy conservation, heat shock proteins, and translational proteins, as previously described (24) (Fig. 3C; see also Table S2B at https://doi.org/10.6084/m9.figshare.12315212). For the ΔsakA proteome, the results showed enrichment in down-regulated proteins involved in glycolysis and gluconeogenesis (7 proteins) and C-compound and carbohydrate metabolism (23 proteins) (see Table S3A).

These data indicate that control of proteins involved in metabolism, such as in production of secondary metabolites, was highly represented in both mutants, suggesting that both kinases were under the control of production of metabolites as a response to caspofungin stress.

Analysis of ΔmpkA and ΔsakA phosphoproteome under the control of the fungal response to caspofungin stress. Results of phosphoproteomic analysis of mutants versus wild-type strain indicated a total of 1,217 and 1,235 phosphopeptides showing statistically significant differences in comparisons of the ΔmpkA mutant to the WT strain (ΔmpkA/WT) or ΔsakA/WT, respectively, during 1 h of incubation with 2 μg/ml caspofungin (Fig. 3A and B; see also Tables S2B and S3B at https://doi.org/10.6084/m9.figshare.12315212). A total of 245 phosphoproteins were found to be shared among the wild-type, ΔmpkA, and ΔsakA strains (Fig. 3B; see also Tables S1, S2B, and S3B). A total of 137 phosphoproteins were unique to the ΔmpkA mutant, while 88 were unique to the ΔsakA mutant (Fig. 3B; see also Tables S2B and S3B). There was a predominant decrease in phosphorylation seen for both mutants in comparison with the WT strain. Most (>75%) of the phosphosites identified were serine residues followed by threonine residues and a minimal percentage of tyrosine residues (Fig. 3C). Most of the phosphopeptides were found to have one phosphorylation site per peptide, but four phosphorylation sites per peptide were observed in a few cases (Fig. 3D).

The results of the functional categorization of phosphopeptides from both mutants were very similar and showed a high number of proteins with decreased phosphorylation involved in budding, cell polarity, and filament formation; Ca²⁺-mediated signal transduction; cellular signaling; cytokinesis (cell division)/septum formation and hydrolysis;

A.

| MAPKs mutants response to 2 µg / mL Caspofungin for 1 h	Proteome		Phosphoproteome	
	ΔsakA	ΔmpkA	ΔsakA	ΔmpkA
Total protein/phosphopeptide p<0.05	101	626	1217 (645)	1235 (703)
Protein/phosphopeptide only in WT 2 (total dephosphorylation)	11	5	348	309
Protein/phosphopeptide only in mutant 2 (total phosphorylation)	0	60	25	76
Protein/phosphopeptide present in both with increase of intensity	18	334	3	49
Protein/phosphopeptide present in both with decrease of intensity	72	227	841	801
Common proteins in proteome for both mutants	53		-	-
Common phosphopeptides in phosphoproteome for both mutants	-	-	501	
Common proteins with WT	11	37	-	-
Common phosphopeptides with WT	-	-	301	310
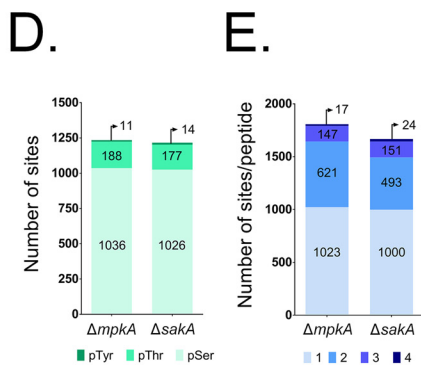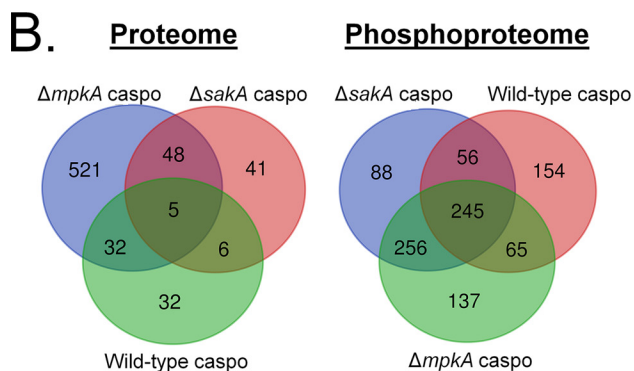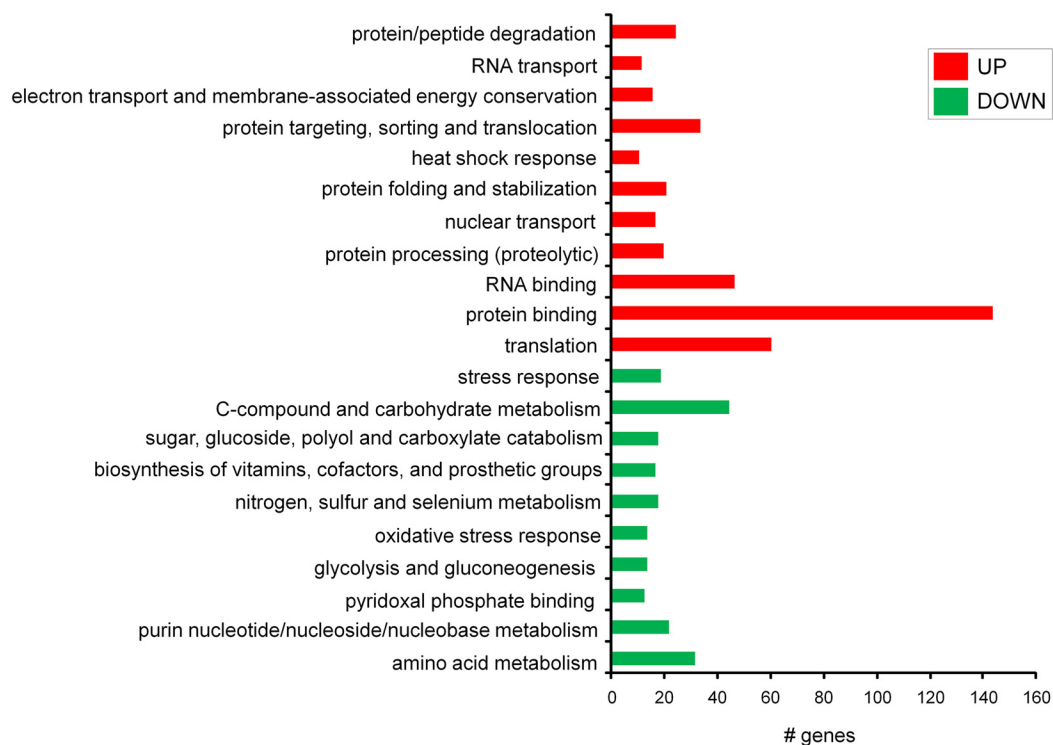
FIG 3 *A. fumigatus* ΔmpkA and ΔsakA proteomic and phosphoproteomic analysis. (A) Summary table of all proteins and phosphopeptides with difference in intensity between mutant samples (ΔmpkA and ΔsakA strains) and the wild-type strain after 2 µg/ml caspofungin treatment for 1 h ($P < 0.05$). (B) Venn diagram of proteins (proteomes) and phosphopeptides with difference in intensity between mutant (ΔmpkA caspo and ΔsakA caspo) samples and WT samples and between wild-type samples after 2 µg/ml caspofungin treatment for 1 h and WT samples at time zero (T0) ($P < 0.05$). (C) Functional enrichment was performed with FungiFun (https://sbi.hki-jena.de/fungifun/fungifun.php), using *A. fumigatus* Af293 as the organism and FunCat as the ontology classification. (D) Number of phosphorylated residues of serine, threonine, or tyrosine identified after phosphoproteomic analysis for both mutant strains. (E) Number of sites of phosphorylation per peptide for both mutant strains.

the MAPKKK cascade; the mitotic cell cycle; cell cycle control; modification by phosphorylation, dephosphorylation, and autophosphorylation; small-GTPase-mediated signal transduction; and transcriptional control (Fig. 4; see also Table S2B and C). In addition, the Δ*sakA* mutant showed decreased phosphorylation of proteins involved in nucleotide/nucleoside/nucleobase binding, regulation of C-compound and carbohydrate metabolism, and RNA synthesis (Fig. 4B; see also Table S2B at https://doi.org/10.6084/m9.figshare.12315212).

Taken together, these data strongly suggest that MpkA and SakA collaborate in orchestrating the global phosphorylation of several proteins involved in the response to caspofungin.

Kinases and transcription factors are involved in the fungal response to caspofungin. Our major interest is in the identification of kinases and transcription factors that may be regulated in *A. fumigatus* during caspofungin responses, which might be under the control of fungal MAPKs. There are 28 kinases modulated in the wild-type strain (Tables 1 and 2). A total of 44 kinases were identified in WT, Δ*mpkA*, and Δ*sakA* samples treated with caspofungin (Table 1). Fourteen kinases were common for all of the strains, 12 kinases were common between the two null mutant strains, and 28 kinases were found to be modulated only during the WT response to caspofungin (Table 1). Table 2 shows the distribution of phosphopeptides in the MAP kinases from the three different MAP kinase modules in the wild-type, Δ*mpkA*, and Δ*sakA* strains upon exposure to caspofungin. All three MAP kinases from the cell wall integrity pathway were found to have phosphopeptides with modulated phosphorylation in the presence of caspofungin (Table 2). MAPKKK SskB and MAPK SakA in the HOG pathway and only the MAPKKK SteC in the invasive growth pathway were also found to have phosphopeptides with modulated phosphorylation (Table 2). Among the kinases exclusively associated with the WT strain, BckA (AFUA_3G11080) is an example of a protein with modulation of two different peptides, one with one site of increased phosphorylation (indicated in bold highlighting) (ESQAPSEGAPDT**S**PK) and a second one with two sites with dephosphorylation (indicated in bold highlighting) (SPRPQDD**S**DED**S**DDGLFAIPLSNNK) (Table 2; see also Table S1B at https://doi.org/10.6084/m9.figshare.12315212). The positions of the phosphopeptides indicate that S1039 and S1043 are closer to the active site of the kinase whereas S376 is closer to the N terminus of BckA. The S1039 residue can be phosphorylated by CKII, while the S1043 residue can be a substrate of CKI and CKI I (see Table S1B).

The phosphorylation profiles determined for kinases of the strains after exposure to caspofungin changed dramatically (Tables 1 and 2). In the wild-type strain, most of the kinases showed decreased phosphorylation compared to the untreated control, except for the mitogen-activated protein kinases SskB[Ssk2] (AFUA_1G10940), SakA-[Hog1] (AFUA_1G12940), and Kic1 (AFUA_2G13640). There was also decreased phosphorylation seen in both the Δ*mpkA* mutant (except for AFUA_2G09570 and AFUA_7G03720, Kin28) and the Δ*sakA* mutant (Tables 1 and 2). To obtain insight into the integrated kinase signaling networks governing caspofungin phosphoproteomics, we generated functional gene networks using STRING analysis. The protein kinase interaction network generated for the wild-type strain showed not only the MAP kinase subnetwork (SakA[Hog1], SskB[Ssk2], SteC[Ste11], BckA[Bck1], and MpkA[Mpk1]) but also the cAMP-dependent protein kinases PkaR[Pka1] and SchA[Sch9] as highly connected (Fig. 5A). Although PkaR[Pka1] was still present in the Δ*mpkA* and Δ*sakA* protein kinase interaction network, most of the MAP kinases and SchA[Sch9], as well as the corresponding associated proteins, were not present (Fig. 5B and C). These results strongly indicate that MpkA and SakA have an important influence on global phosphorylation during caspofungin tolerance.

There was also a great difference seen in the phosphorylation profiles generated for transcription factors (TFs) among strains postexposure to caspofungin (Table 3). In the wild-type strain, most of the TFs showed decreased phosphorylation compared to the untreated control, except for Sin3 (AFUA_8G05570). There was also decreased phosphorylation in both the Δ*mpkA* mutant (except for AFUA_6G09930, Yap1, and AFUA_3G13920, Mbp1) and the Δ*sakA* mutant (Table 3). As a first step in characterizing

A.

Phosphoproteome Δ*mpkA* caspo / wild-type caspo
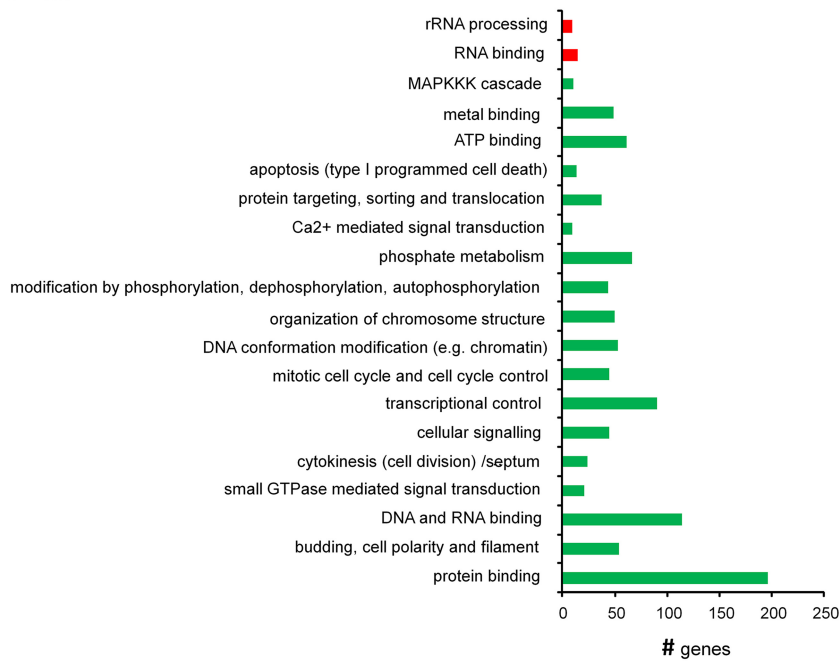
B.

Phosphoproteome Δ*sakA* caspo / wild-type caspo

UP
DOWN
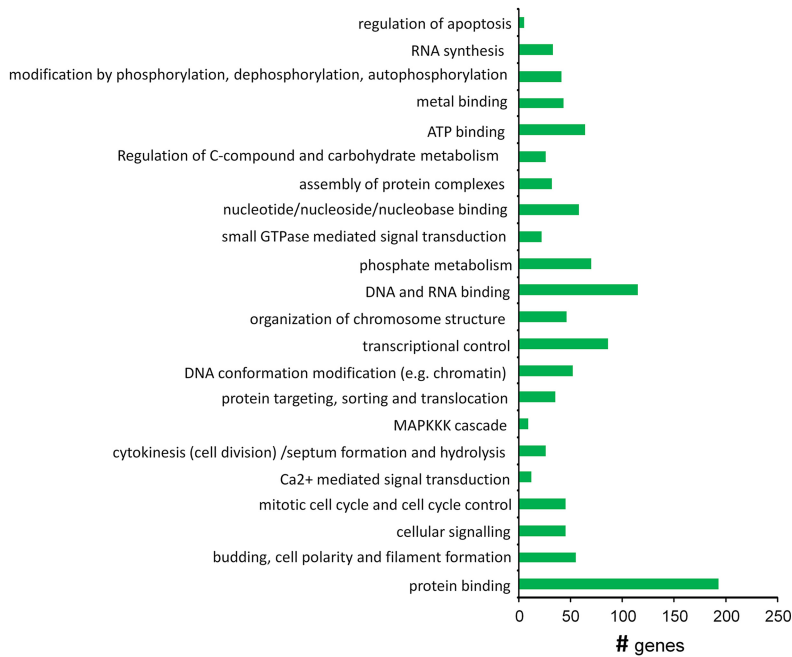
FIG 4 Phosphoproteome functional categorization of *A. fumigatus* Δ*mpkA* and Δ*sakA* mutants. Functional categorization of phosphopeptides differentially phosphorylated in the Δ*mpkA* strain ($P < 0.05$) (A) or Δ*sakA* strain ($P < 0.05$) (B) was performed. Functional enrichment was performed with FungiFun (https://sbi.hki-jena.de/fungifun/fungifun.php), using *A. fumigatus* Af293 as the organism and FunCat as the ontology classification.

TABLE 1 Protein kinases with modulation of phosphorylation

Gene ID	Gene name	Protein name	Modulation[a]		
			WT caspo/ control	ΔmpkA caspo/ WT caspo	ΔsakA caspo/ WT caspo
AFUA_3G12670	pkh2[b]	Serine/threonine protein kinase, putative	↓ ↑	↓	↓
AFUA_6G06870	yck2[b]	Casein kinase I homolog, putative	↑	↓	↓
AFUA_5G03160	ctk1[b]	Protein kinase, putative	↓	↓ ↓	↓ ↓
AFUA_1G09950	cbkA	Casein kinase II subunit beta (CK II beta)	↓	↓	↓
AFUA_5G11520	nrc2	Serine/threonine protein kinase (Nrc-2), putative (EC 2.7.1.-)	↓	↓	↓
AFUA_5G05980	tos3[b]	Calcium/calmodulin dependent protein kinase, putative	↓ ↓	↓	↓
AFUA_1G14810	kin4	Serine/threonine protein kinase (Kin4), putative (EC 2.7.11.1)	↓	↓	↓
AFUA_2G12210	sin1	Stress-activated MAP kinase interacting protein, putative	↓	↓	↓
AFUA_3G10000	pkaR	cAMP-dependent protein kinase regulatory subunit (PKA regulatory subunit)	↓	↓	↓ ↓
AFUA_2G01700	snf1[b]	Nonspecific serine/threonine protein kinase (EC 2.7.11.1)	↓	↓ ↓ ↓	↓ ↓ ↓ ↓
AFUA_5G11840	hrk1[b]	Protein kinase, putative (EC 2.7.1.-)	↓	↓	↓ ↓
AFUA_2G15010	srrB[c]	Serine threonine protein kinase, putative	↓	↓ ↓	↓ ↓
AFUA_1G11080	kin1	Nonspecific serine/threonine protein kinase (EC 2.7.11.1)	↓ ↓ ↓ ↓	↓	↓
AFUA_6G08120	sldA	Checkpoint protein kinase (SldA), putative	↓	↓	↓
AFUA_2G14200	prr1[b]	Protein kinase, putative	−	↓ ↓	↓
AFUA_7G04330	ste20[c]	Ste20-like serine/threonine protein kinase, putative	−	↓	↓
AFUA_1G11930	nnk1[b]	Serine/threonine-protein kinase, putative	−	↓	↓
AFUA_3G08710	isr1[c]	Protein kinase domain-containing protein	−	↓	↓
AFUA_4G08920	iks1[b]	Protein kinase, putative	−	↓	↓
AFUA_4G06180	ckb1[b]	Casein kinase II subunit beta	−	↓	↓
AFUA_5G11970	pkcA	Protein kinase C	−	↓	↓
AFUA_6G04500	gal83[b]	Snf1 kinase complex beta-subunit Gal83, putative	−	↓ ↓	↓
AFUA_6G09240	ypk2[b]	Protein kinase	−	↓	↓
AFUA_1G16780	lkh1	Protein kinase (Lkh1), putative	−	↓	↓
AFUA_1G05800	mkk2	MAP kinase kinase (Mkk2), putative	−	↓	↓
AFUA_6G05120	skp1	Glycogen synthase kinase (Skp1), putative	↓	↓	−
AFUA_4G13720	mpkA	(MpkA) mitogen-activated protein kinase (EC 2.7.11.24)	↓ ↓	−	−
AFUA_2G13640	kic1[b]	Serine/threonin protein kinase, putative	↑	↓	−
AFUA_1G12940	sakA	(SakA) mitogen-activated protein kinase hog1 (MAP kinase hog1) (EC 2.7.11.24)	↑	−	−
AFUA_2G11730	gin4[b]	Protein kinase domain-containing protein	↓	−	−
AFUA_2G16620	gcn2[b]	Protein kinase, putative	↓	−	−
AFUA_4G01020	fhk1	Sensor histidine kinase/response regulator, putative (AFU_orthologue AFUA_4G01020)	↓	−	−
AFUA_7G03750	cds1	Serine/threonine-protein kinase chk2 (Cds1)	↓ ↓ ↓ ↓	−	−
AFUA_1G10940	sskB	MAP kinase kinase kinase (EC 2.7.11.-)	↑	−	−
AFUA_4G03140	sky1	Serine protein kinase Sky1, putative (EC 2.7.1.-)	↓ ↓	−	−
AFUA_1G06400	schA	Nonspecific serine/threonine protein kinase (EC 2.7.11.1)	↓	−	−
AFUA_5G06420	steC	MAP kinase kinase kinase SteC (EC 2.7.1.-)	↓	−	−
AFUA_3G11080	bck1	MAP kinase kinase kinase (Bck1), putative	↓ ↓ ↓	−	−
AFUA_2G01520	yak1[b]	Protein kinase, putative	↓	−	−
AFUA_2G09570	stk-55[d]	Serine/threonine protein kinase	−	↑	−
AFUA_2G10620	ypk1	Serine/threonine protein kinase (YPK1), putative	−	↓	−
AFUA_7G03720	kin28	Serine/threonine protein kinase (Kin28), putative	−	↑	−
AFUA_1G05930	prk1[b]	Serine/threonine protein kinase, putative	−	−	↓ ↓
AFUA_2G04680	pakA	Nonspecific serine/threonine protein kinase (EC 2.7.11.1)	−	−	↓

[a]The number of arrows represents the number of phosphopeptides identified for each protein (an arrow pointing down [↓] represents a phosphopeptide that has decreased phosphorylation whereas an arrow pointing up [↑] represents a phosphopeptide that has increased phosphorylation). −, the protein was not found under the described conditions.
[b]Gene name of orthologs in *S. cerevisiae*.
[c]Gene name of orthologs in *A. nidulans*.
[d]Gene name of orthologs in *N. crassa*.

the influence of these TFs on caspofungin tolerance, we analyzed the ability of 13 null mutants of these TFs (29) to grow on caspofungin. We previously observed that a ΔhapB mutant (AFUA_2G14720, encoding a CAAT-binding TF) (30) and a ΔatfA mutant (AFUA_3G11330) were more susceptible to caspofungin at 0.2 μg/ml than the wild-type strain and showed reduced CPE (Fig. 6). A ΔpacC mutant (AFUA_3G11970, encoding a TF that undergoes activation in response to alkaline pH) (31), and a ΔzipD mutant (AFUA_2G03280, encoding a TF important for calcium metabolism and osmotic response) (9, 10), were previously found to have reduced CPE.

TABLE 2 Phosphopeptides observed as differentially modulated in the presence of caspofungin in the mitogen-activated protein kinases[a]

Pathway and MAPK	WT caspo/ WT control	ΔmpkA caspo/ WT caspo	ΔsakA caspo/ WT caspo	Phosphopeptide
Cell wall integrity				
MAPKKK BckA (AFUA_3G11080)	Up (2.92)			364-ESQAPSEGAPDTSPK-378
		Down (0.28)		364-ESQAPSEGAPDTSPK-378
			Down (0.26)	364-ESQAPSEGAPDTSPK-378
		Down (0.08)		379-LSHEPQSAGPHSGTIENSPNLR-400
		Down		798-DAPQHTEGMSPVEGDQQVGISPEPDKADLLAR-829
			Down (0.26)	798-DAPQHTEGMSPVEGDQQVGISPEPDKADLLAR-829
	Down (0.47)			1032-SPRPQDDSDEDSDDGLFAIPLSNNK-1056
		(Down) 0.31		1032-SPRPQDDSDEDSDDGLFAIPLSNNK-1056
			Down	1032-SPRPQDDSDEDSDDGLFAIPLSNNK-1056
MAPKK Mkk2 (AFUA_1G05800)		(Down) 0.30		92-PAPPPLATTGLNESTGHSR-110
			Down	92-PAPPPLATTGLNESTGHSR-110
MAPK MpkA (AFUA_4G13720)	Down (0.12)			173-GFSIDPEENAGYMTEYVATR-192
	Down (0.16)			173-GFSIDPEENAGYMTEYVATR-192
		Up		173-GFSIDPEENAGYMTEYVATR-192
Invasive growth				
MAPKKK SteC (AFUA_5G06420)	Down			584-DSIASSSLQPLQEESPIEPNRK-605
High-osmolarity glycerol				
MAPKKK SskB (AFUA_1G10940)	Up			118-GSSVGAGAALDKVSPVDGLPLTDR-141
		Down (0.04)		118-GSSVGAGAALDKVSPVDGLPLTDR-141
MAPK SakA (AFUA_1G12940)	Up (1.8)			165-IQDPQMTGYVSTR-177

[a]"Down" and "Up" represent decreased and increased phosphorylation of a specific phosphopeptide, respectively. Numbers in parentheses represent fold change. MAPK, mitogen-activated protein kinase.

DISCUSSION

Echinocandins, including caspofungin, anidulafungin, and micafungin, represent the second line of treatment for invasive aspergillosis (32, 33). Echinocandins act by the inhibition of the protein Fks1, a component of fungal membrane, resulting in the disruption of the synthesis of the polysaccharide β-(1,3) glucan, a major component of the fungal cell wall (33). In this work, we performed proteome and phosphoproteome analyses of a WT strain and of MAPK null mutants (the ΔmpkA and ΔsakA strains) under conditions of high caspofungin concentrations in liquid medium, aiming to identify new targets related to the CPE in *A. fumigatus*. For the analysis of wild-type responses to caspofungin, we identified 814 phosphopeptides (520 unique proteins) with modulation of phosphorylation. Most of the phosphopeptides suffered a decrease of phosphorylation, with a predominance of proteins being related to transcriptional control. The analysis of the response of the ΔmpkA strain to caspofungin indicates that 1,235 phosphopeptides were being modulated (703 unique proteins), most of them with decreased phosphorylation, such as was observed for the WT response to caspofungin. The modulation of proteins involved in transcriptional control and phosphate metabolism was predominant, as was also observed for the ΔsakA phosphoproteome.

The participation of MpkA and SakA in the caspofungin response is well established (6, 9, 16, 27). Activation of CWI pathways, together with increased MpkA phosphorylation, occurs at lower concentrations of caspofungin (9). However, under conditions of high concentrations, the phosphorylation of the kinase is reduced (9). In addition, it is known that chitin biosynthesis in *Candida albicans* can be modulated by components of the high-osmolarity glycerol (HOG) pathway (7). It has also been demonstrated that, in *A. fumigatus* treated with subinhibitory concentrations of caspofungin, an *in silico* interaction may occur between SakA and MpkA (16). Here, we showed the involvement of MpkA and SakA in the modulation of phosphorylation of different targets during the response to high doses of caspofungin. We observed that MpkA and SakA suffered dephosphorylation and phosphorylation, respectively, when the wild-type strain was exposed to caspofungin.

Modulation of protein kinases and transcription factors in the response to caspofungin stress was highly represented in all analyses performed. The protein kinase A
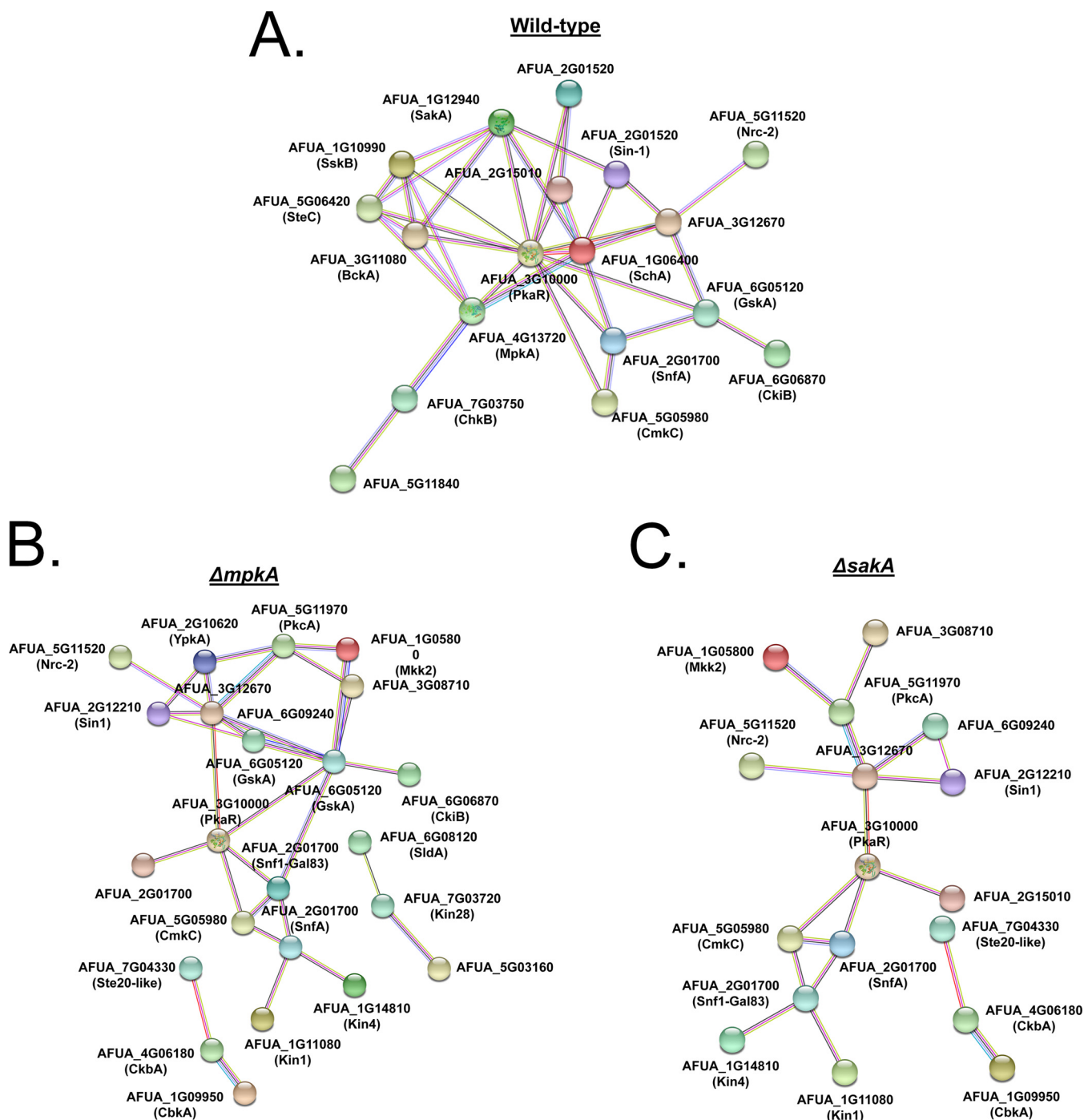
FIG 5 *A. fumigatus* protein kinase functional protein association network based on the protein phosphorylation profile during incubation with caspofungin. The sets of differentially protein kinase phosphorylated proteins from the wild-type (WT) (A), ΔmpkA (B), and ΔsakA (C) strains during caspofungin stress were combined for the generation of a general protein association network. Each edge represents a functional protein association retrieved from the STRING server (medium confidence threshold of 0.4 for the interaction score), and node sizes represent the degree of each node (number of edges connected to the node). Note that not all the differentially phosphorylated proteins are present in the network as many proteins did not present any functional associations within the whole set.

(PKA) regulatory subunit (AFUA_3G10000), for example, showed decreased phosphorylation (site indicated in bold highlighting) in the wild-type strain exposed to caspofungin (site RT**S**VS, ratio = 0.5), which was also observed in ΔmpkA and ΔsakA phosphoproteomes. In the MAPK null mutant strains, four sites of phosphorylation (indicated with bold highlighting) were identified with dephosphorylation (for the

TABLE 3 Transcription factors with modulation of phosphorylation

Gene ID	Gene name	Protein name	Modulation[a]		
			WT caspo/ control	ΔmpkA caspo/ WT caspo	ΔsakA caspo/ WT caspo
AFUA_3G11970	pacC	C2H2 transcription factor PacC, putative	↓	↓	↓
AFUA_3G11330	atfA	BZIP transcription factor (AtfA), putative	↓	↓	↓
AFUA_1G09670	glcD	HLH transcription factor (GlcD gamma), putative	↓	↓	−
AFUA_3G02340	ncb2[b]	CBF/NF-Y family transcription factor, putative	↓	−	↓
AFUA_2G14720	hapB	CCAAT-binding transcription factor subunit HAPB	↓↓↓	−	↓↓↓
AFUA_2G03280	zipD	BZIP transcription factor, putative	−	↓↓	↓↓
AFUA_2G01900	rtf1p	RNA polymerase II transcription elongation factor Rtf1p, putative	−	↓	↓
AFUA_1G12332	rph1[b]	Jumonji family transcription factor, putative	−	↓	↓
AFUA_2G13380	areB	GATA transcription factor (AreB), putative	−	↓	↓↓
AFUA_3G11170	csp-2[c]	CP2 transcription factor, putative	−	↓↓↓	↓
AFUA_2G14250	bur6[b]	CBF/NF-Y family transcription factor, putative	−	↓	↓
AFUA_1G12260	iws1	Transcription factor iws1	−	↓	↓
AFUA_5G11390	bqt4[d]	APSES transcription factor, putative	−	↓↓↓↓	↓↓
AFUA_3G08520	rlmA	SRF-type transcription factor RlmA	−	↓	↓
AFUA_5G13310	aro80[b]	C6 transcription factor, putative	−	↓	↓
AFUA_8G05570	sin3	Transcription factor (Sin3), putative	↑	−	−
AFUA_1G10760	mak21[b]	CCAAT-box-binding transcription factor	↓↓	−	−
AFUA_7G04710	fap1[b]	NF-X1 finger transcription factor, putative	↓	−	−
AFUA_3G11960	fkh2[b]	Forkhead transcription factor Fkh1/2, putative	↓↑	−	−
AFUA_1G06900	crzA	C2H2 finger domain transcription factor CrzA	↓	−	−
AFUA_2G17220	amdX	C2H2 transcription factor (AmdX), putative	↓	−	−
AFUA_2G14800	hpa3	HLH transcription factor (HpaIII), putative	↓	−	−
AFUA_5G03430	rum1	PHD transcription factor (Rum1), putative	↓	−	−
AFUA_6G09930	yap1	BZIP transcription factor AP-1/Yap1, putative	−	↑	−
AFUA_3G13920	mbp1[b]	APSES transcription factor, putative	−	↓↓	−
AFUA_7G05620	mpbA	APSES transcription factor (MbpA), putative	−	↑	−
AFUA_5G04190	palcA	HLH transcription factor (PalcA), putative	−	−	↓

[a]The number of arrows represents the number of phosphopeptides identified for each protein (an arrow pointing down [↓] represents a phosphopeptide that has decreased phosphorylation whereas an arrow pointing up [↑] represents a phosphopeptide that has increased phosphorylation). −, the protein was not found under the described conditions.
[b]Gene name of ortholog in *S. cerevisiae*.
[c]Gene name of ortholog in *N. crassa*.
[d]Gene name of ortholog in *S. pombe*.

ΔsakA phosphoproteome, sites KY**S**PI [ratio = 0], RT**S**VS [ratio = 0.12] VT**S**PT [ratio = 0.13], and P**S**PS [ratio = 0.28]; for the ΔsakA phosphoproteome, sites P**S**PS [ratio = 0], KY**S**PI [ratio = 0], VT**S**PT [ratio = 0.03], and RT**S**VS [ratio = 0.06]). There is a physical interaction between *A. fumigatus* SakA and MpkC (17, 34) and the PKA
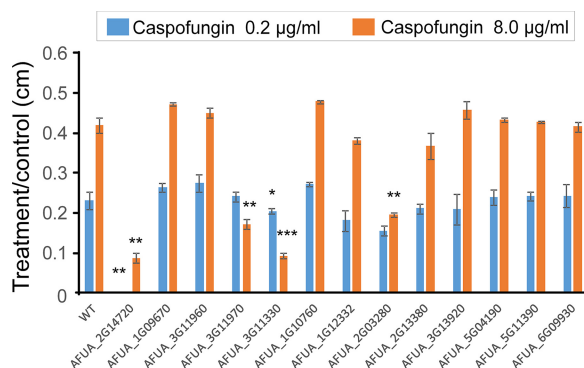

FIG 6 Analysis of *A. fumigatus* null TF strains grown on different concentrations of caspofungin. (A) *fumigatus* conidia (1×10^5) were inoculated on solid minimal medium (MM) with different concentrations of caspofungin and grown for 5 days at 37°C. All plates were grown in triplicate, and averages ± standard deviations (SD) of data were plotted. A Student *t* test was performed using Prism GraphPad (version 6) to confirm the statistical significance of differences between treatment and control results (*, $P < 0.05$, **, $P < 0.01$; ***, $P < 0.001$).

regulatory subunit (35). Carbohydrate mobilization is controlled by SakA interactions with PkaC1 catalytic and PkaR regulatory subunits, suggesting a putative mechanism where the PkaR regulatory subunit leaves the complex and releases the SakA-PkaC1 complex for activation of enzymes involved in carbohydrate mobilization (35). These results suggest a possible participation of PKA, CWI, and HOG pathways in the mobilization of carbohydrate for cell wall remodeling and for responses to caspofungin. In addition, the importance of PKA in fungal viability was also observed in strains deleted for *pkaC1*, which suffered defects in germination and in cell wall organization (36–38). Here, protein kinase C (PKC; AFUA_5G11970) was also identified with dephosphorylation in both the Δ*mpkA* and Δ*sakA* mutant strains. PKC acts in the CWI pathway in *Saccharomyces cerevisiae* and *A. fumigatus* by the activation of MAPKs with involvement of Bck1 (a MAPKKK, dephosphorylated in WT caspofungin samples), Mkk1/Mkk2 (Mkk2 [AFUA_1G05800], with dephosphorylation in both null mutant strains), and MpkA (AFUA_4G13720, with dephosphorylation only in the WT) (39–43).

Some transcription factors identified here have already been shown to be related to CPE in *A. fumigatus*, such as AtfA (AFUA_3G11330), a homologue of ATF1 (which also includes AtfB or AtfD) (14), with dephosphorylation in the WT, Δ*mpkA*, and Δ*sakA* strains. The ZipD transcription factor (AFUA_2G03280), with dephosphorylation in both mutant strains, also plays a role in the caspofungin-induced CWI response pathway (9, 10). AreB (AFUA_2G13380), with a decrease of phosphorylation in both null mutant strains, was also identified with a modulation of phosphorylation in *A. fumigatus* responses to Congo red (25).

In our study, we demonstrated the complexity of the fungal response to caspofungin stress. The members of the main group of proteins with strong modulation of phosphorylation are related to the transcription control, followed by proteins related to phosphate metabolism and transfer, in which kinases were highly represented. However, the modulation of proteins related to cytoskeletal organization and heat shock responses and β-1,3-glucan synthase is also important; in addition to calcium-calcineurin pathway and CWI pathways, all of them have already been described in the literature as important for the CPE in *A. fumigatus* and other fungi (7, 8, 10, 19, 28, 44, 45).

Increased understanding of how the modulation of protein phosphorylation may affect the fungal growth in the presence of caspofungin represents an important step in the development of new strategies and methods to combat the fungus inside the host. We showed that the phosphorylation profile is strongly modulated during the drug response, which can be also related to groups of proteins that have already been identified and described as showing level changes during the CPE response (28, 46). We have also shown that the MAPKs MpkA and SakA may control the CPE response by the modulation of the phosphorylation of new targets, which deserves further investigation by future studies.

MATERIALS AND METHODS

Fungal growth, protein extraction, digestion, and phosphoenrichment. *Aspergillus fumigatus* conidia (1×10^7) from the wild-type (WT) strain and mutant strains (Δ*mpkA* and Δ*sakA* mutants) (strain details are shown in Table S11 at https://doi.org/10.6084/m9.figshare.12315212) were inoculated into YG medium {0.5% yeast extract, 1% dextrose, 0.1% trace elements [22.0 g/liter $ZnSO_4$, 11 g/liter boric acid, 5 g/liter $MnCl_2$, 5 g/liter $FeSO_4$, 1.6 g/liter $CoCl_2$, 1.6 g/liter $CuSO_4$, 1.1 g/liter $(NH4)_2MoO_4$]} and incubated for 16 h with rotation at 200 rpm at 37°C. After growth of mycelia, 2 μg/ml of caspofungin was added to the flasks, followed by incubation for 1 h. Mycelia were filtered using a vacuum system, harvested, and frozen by the use of liquid nitrogen. Frozen mycelia were macerated, resuspended in 1 ml TNE buffer (50 mM Tris-HCl [pH 7.5], 140 mM NaCl, 5 mM EDTA, EDTA-free protease inhibitor cocktail [Roche], 0.1 mM phenylmethylsulfonyl fluoride [PMSF], 100 mM NaF, 1 mM Na_3VO_4, 0.05 mM sodium β-glycerophosphate) and incubated for 15 min with agitation following centrifugation at 13,000 × *g* for 10 min. The supernatant was collected and total protein quantified Bradford assay (47). A 500-μg volume of protein was precipitated by addition of trichloroacetic acid (TCA) at a final 10% (wt/vol) concentration, subjected to vortex mixing for 15 s, and placed on ice for a minimum of 30 min. Samples were centrifuged at 14,000 × *g* for 15 min, and the supernatant was discarded. The pellet was washed three times with cold acetone with centrifugation at 14,000 × *g* (4°C) for 10 min. Proteins were dissolved in 150 μl of 8 M urea and 50 mM ammonium bicarbonate (Ambic). Dithiothreitol (DTT) (10 mM) was added followed by incubation for 45 min at 30°C. Protein alkylation was performed by addition of 40 mM

iodoacetamide and incubation for 30 min at room temperature in the dark; 5 mM DTT was added with 15 min of incubation at 30°C. Ambic (50 mM) was added for urea dilution, and trypsin was added at a trypsin/protein ratio of 1:50. Protein digestion was performed by an overnight (16-h) incubation at 30°C. The digestion was stopped by addition of trifluoroacetic acid (TFA) to reach a final concentration of 1%. Samples were desalted by the use of an Oasis MCX Plus short cartridge (Waters), and peptide concentrations were determined by the use of a Qubit protein assay kit (Thermo Fisher Scientific). From the total peptides, 5% was collected for proteomic analysis, and 95% was used for phosphopeptide enrichment with TiO_2 resin (Titansphere; GL Sciences Inc., Japan) in batch mode. Samples were resuspended in 80% acetonitrile (ACN)–1 M glycolic acid–5% TFA and mixed into the resin (1 mg resin to 500 μg peptide) and incubated for 20 min at room temperature. Resin was washed three times with 80% ACN–1% TFA, and phosphopeptides were eluted with 0.5% NH_4OH (48, 49).

Nano-LC-MS/MS (nano-liquid chromatography–tandem mass spectrometry) analysis. Peptide samples were resuspended in 0.1% formic acid (FA) before analysis using a nano-flow EASY-nLC 1200 system (Thermo Scientific) coupled to an Orbitrap Fusion Tribrid mass spectrometer (Thermo Scientific) (Instituto de Química, Universidade de São Paulo). The peptides were loaded on an Acclaim PepMap C_{18} (Thermo Scientific, Germany) trap column (2 cm in length, 100-μm inner diameter; 5-μm pore size) and separated onto an Acclaim PepMap C_{18} (15 cm in length, 75-μm inner diameter; 3-μm pore size) column and separated with a gradient from 100% mobile phase A (0.1% FA) to 28% phase B (0.1% FA, 80% ACN) for 70 min, 28% to 40% for 10 min, and 40% to 95% for 2 min and 12 min at 95% at a constant flow rate of 300 nl/min. The mass spectrometer was operated in positive-ion mode with data-dependent acquisition. The full scan was acquired in the Orbitrap instrument at a resolution of 120,000 FWHM (full width at half-maximum) in the 375 to 1,600 m/z mass range with a maximum injection time of 50 ms and an automatic gain control (AGC) target of 5E−5. Peptide ions were selected using the quadrupole with an isolation window of 1.2 and were fragmented with high-energy collisional dissociation (HCD) MS/MS using a normalized collision energy value of 35 and were detected in the ion trap. Data-dependent acquisition performed with a cycle time of 3 s was used to select the precursor ions for fragmentation. Dynamic exclusion was activated with 12 s as exclusion duration and 20 ppm as the mass tolerance. All raw data were accessed in Xcalibur software (Thermo Scientific).

Database searches and bioinformatics analyses. Raw data were processed using MaxQuant software version 1.5.2.8 and the embedded database search engine Andromeda. The MS/MS spectra were searched against the UniProt *Aspergillus fumigatus* Protein Database (downloaded October 2017; 9,648 entries), with the addition of common contaminants, with accuracies of 4.5 ppm for MS and 0.5 Da for MS/MS. Cysteine carbamidomethylation (57.021 Da) was set as the fixed modification, with two missed cleavages for trypsin. Methionine oxidation (15.994 Da), protein N-terminal acetylation (42.010 Da), and phosphorylation S/T/Y (+79.96 Da) were set as variable modifications. Proteins and peptides were accepted at a false-discovery rate (FDR) of less than 1%. Label-free quantification was performed using MaxQuant software with the "match between run" and iBAQ features activated. The levels of MS intensity of phosphopeptides determined under the different conditions were compared, and the Student t test was used for the comparisons. Three biological replicates for each strain were analyzed. Plots of results of principal-coordinate analysis (PCA) comparing all untreated replicates (control) and caspofungin (2 μg/ml)-treated replicates, for proteome or phosphoprotrome samples, are indicated in Fig. S1 (available at https://doi.org/10.6084/m9.figshare.12315212).

The functional enrichment was performed with FungiFun (https://sbi.hki-jena.de/fungifun/fungifun .php), using *A. fumigatus* Af293 as the organism, FunCat as the ontology classification, and identifiers (IDs) from each supplemental table (only "AFUA_" IDs were used).The protein-protein interaction networks were obtained by the use of STRING (https://string-db.org/) and Cytoscape version 3.6.1.

REFERENCES

1. Robbins N, Wright GD, Cowen LE. 2016. Antifungal drugs: the current armamentarium and development of new agents. Microbiol Spectr 4(5). https://doi.org/10.1128/microbiolspec.FUNK-0002-2016.
2. Valiante V, Macheleidt J, Foge M, Brakhage A. 2015. The *Aspergillus fumigatus* cell wall integrity signaling pathway: drug target, compensatory pathways, and virulence. Front Microbiol 6:325. https://doi.org/10.3389/fmicb.2015.00325.
3. Walsh TJ, Anaissie EJ, Denning DW, Herbrecht R, Kontoyiannis DP, Marr KA, Morrison VA, Segal BH, Steinbach WJ, Stevens DA, van Burik JA, Wingard JR, Patterson TF, Infectious Diseases Society of America. 2008. Treatment of aspergillosis: clinical practice guidelines of the Infectious

Diseases Society of America. Clin Infect Dis 46:327–360. https://doi.org/10.1086/525258.
4. Arendrup MC, Mavridou E, Mortensen KL, Snelders E, Frimodt-Møller N, Khan H, Melchers WJ, Verweij PE. 2010. Development of azole resistance in *Aspergillus fumigatus* during azole therapy associated with change in virulence. PLoS One 5:e10080. https://doi.org/10.1371/journal.pone.0010080.
5. Stevens DA, White TC, Perlin DS, Selitrennikoff CP. 2005. Studies of the paradoxical effect of caspofungin at high drug concentrations. Diagn Microbiol Infect Dis 51:173–178. https://doi.org/10.1016/j.diagmicrobio .2004.10.006.
6. Steinbach WJ, Lamoth F, Juvvadi PR. 2015. Potential microbiological

effects of higher dosing of echinocandins. Clin Infect Dis 61:S669–S677. https://doi.org/10.1093/cid/civ725.

7. Fortwendel JR, Juvvadi PR, Perfect BZ, Rogg LE, Perfect JR, Steinbach WJ. 2010. Transcriptional regulation of chitin synthases by calcineurin controls paradoxical growth of Aspergillus fumigatus in response to caspofungin. Antimicrob Agents Chemother 54:1555–1563. https://doi.org/10.1128/AAC.00854-09.

8. Juvvadi PR, Muñoz A, Lamoth F, Soderblom EJ, Moseley MA, Read ND, Steinbach WJ. 2015. Calcium-mediated induction of paradoxical growth following caspofungin treatment is associated with calcineurin activation and phosphorylation in Aspergillus fumigatus. Antimicrob Agents Chemother 59:4946–4955. https://doi.org/10.1128/AAC.00263-15.

9. Ries LNA, Rocha MC, de Castro PA, Silva-Rocha R, Silva RN, Freitas FZ, de Assis LJ, Bertolini MC, Malavazi I, Goldman GH. 2017. The Aspergillus fumigatus CrzA transcription factor activates chitin synthase gene expression during the caspofungin paradoxical effect. mBio 8:e00705-17. https://doi.org/10.1128/mBio.00705-17.

10. de Castro PA, Colabardini AC, Manfiolli AO, Chiaratto J, Silva LP, Mattos EC, Palmisano G, Almeida F, Persinoti GF, Ries LNA, Mellado L, Rocha MC, Bromley M, Silva RN, de Souza GS, Loures FV, Malavazi I, Brown NA, Goldman GH. 2019. Aspergillus fumigatus calcium-responsive transcription factors regulate cell wall architecture promoting stress tolerance, virulence and caspofungin resistance. PLoS Genet 15:e1008551. https://doi.org/10.1371/journal.pgen.1008551.

11. Rocha MC, Fabri JH, Franco de Godoy K, Alves de Castro P, Hori JI, Ferreira da Cunha A, Arentshorst M, Ram AF, van den Hondel CA, Goldman GH, Malavazi I. 2016. Aspergillus fumigatus MADS-box transcription factor rlmA is required for regulation of the cell wall integrity and virulence. G3 (Bethesda) 6:2983–3002. https://doi.org/10.1534/g3.116.031112.

12. Jung US, Sobering AK, Romeo MJ, Levin DE. 2002. Regulation of the yeast Rlm1 transcription factor by the Mpk1 cell wall integrity MAP kinase. Mol Microbiol 46:781–789. https://doi.org/10.1046/j.1365-2958.2002.03198.x.

13. Bruder Nascimento AC, Dos Reis TF, de Castro PA, Hori JI, Bom VL, de Assis LJ, Ramalho LN, Rocha MC, Malavazi I, Brown NA, Valiante V, Brakhage AA, Hagiwara D, Goldman GH. 2016. Mitogen activated protein kinases SakA (HOG1) and MpkC collaborate for Aspergillus fumigatus virulence. Mol Microbiol 100:841–859. https://doi.org/10.1111/mmi.13354.

14. Pereira Silva L, Alves de Castro P, Dos Reis TF, Paziani MH, Von Zeska Kress MR, Riaño-Pachón DM, Hagiwara D, Ries LN, Brown NA, Goldman GH. 2017. Genome-wide transcriptome analysis of Aspergillus fumigatus exposed to osmotic stress reveals regulators of osmotic and cell wall stresses that are SakAHOG1 and MpkC dependent. Cell Microbiol 19:e12681. https://doi.org/10.1111/cmi.12681.

15. Manfiolli AO, Siqueira FS, Dos Reis TF, Van Dijck P, Schrevens S, Hoefgen S, Föge M, Straßburger M, de Assis LJ, Heinekamp T, Rocha MC, Janevska S, Brakhage AA, Malavazi I, Goldman GH, Valiante V. 2019. Mitogen-activated protein kinase cross-talk interaction modulates the production of melanins in Aspergillus fumigatus. mBio 10:e00215-19. https://doi.org/10.1128/mBio.00215-19.

16. Altwasser R, Baldin C, Weber J, Guthke R, Kniemeyer O, Brakhage AA, Linde J, Valiante V. 2015. Network modeling reveals cross talk of MAP kinases during adaptation to caspofungin stress in Aspergillus fumigatus. PLoS One 10:e0136932. https://doi.org/10.1371/journal.pone.0136932.

17. Manfiolli AO, Mattos EC, de Assis LJ, Silva LP, Ulaş M, Brown NA, Silva-Rocha R, Bayram Ö, Goldman GH. 2019. Aspergillus fumigatus high osmolarity glycerol mitogen activated protein kinases SakA and MpkC physically interact during osmotic and cell wall stresses. Front Microbiol 10:918. https://doi.org/10.3389/fmicb.2019.00918.

18. Loiko V, Wagener J. 2017. The paradoxical effect of echinocandins in Aspergillus fumigatus relies on recovery of the β-1,3-glucan synthase Fks1. Antimicrob Agents Chemother 61:e01690-16. https://doi.org/10.1128/AAC.01690-16.

19. Moreno-Velásquez SD, Seidel C, Juvvadi PR, Steinbach WJ, Read ND. 2017. Caspofungin-mediated growth inhibition and paradoxical growth in Aspergillus fumigatus involve fungicidal hyphal tip lysis coupled with regenerative intrahyphal growth and dynamic changes in β-1,3-glucan synthase localization. Antimicrob Agents Chemother 61:e00710-17. https://doi.org/10.1128/AAC.00710-17.

20. Satish S, Jiménez-Ortigosa C, Zhao Y, Lee MH, Dolgov E, Krüger T, Park S, Denning DW, Kniemeyer O, Brakhage AA, Perlin DS. 2019. Stress-induced changes in the lipid microenvironment of β-(1,3)-d-glucan syn-

thase cause clinically important echinocandin resistance in Aspergillus fumigatus. mBio 10:e00779-19. https://doi.org/10.1128/mBio.00779-19.

21. Lamoth F, Juvvadi PR, Fortwendel JR, Steinbach WJ. 2012. Heat shock protein 90 is required for conidiation and cell wall integrity in Aspergillus fumigatus. Eukaryot Cell 11:1324–1332. https://doi.org/10.1128/EC.00032-12.

22. Lamoth F, Juvvadi PR, Soderblom EJ, Moseley MA, Steinbach WJ. 2015. Hsp70 and the cochaperone StiA (Hop) orchestrate Hsp90-mediated caspofungin tolerance in Aspergillus fumigatus. Antimicrob Agents Chemother 59:4727–4733. https://doi.org/10.1128/AAC.00946-15.

23. Aruanno M, Glampedakis E, Lamoth F. 2019. Echinocandins for the treatment of invasive aspergillosis: from laboratory to bedside. Antimicrob Agents Chemother 63:e00399-19. https://doi.org/10.1128/AAC.00399-19.

24. Aruanno M, Bachmann D, Sanglard D, Lamoth F. 2019. Link between heat shock protein 90 and the mitochondrial respiratory chain in the caspofungin stress response of Aspergillus fumigatus. Antimicrob Agents Chemother 63:e00208-19. https://doi.org/10.1128/AAC.00208-19.

25. Mattos EC, Silva LP, Valero C, de Castro PA, Dos Reis TF, Ribeiro LFC, Marten MR, Silva-Rocha R, Westmann C, da Silva C, Taft CA, Al-Furaiji N, Bromley M, Mortensen UH, Benz JP, Brown NA, Goldman GH. 2020. The Aspergillus fumigatus phosphoproteome reveals roles of high-osmolarity glycerol mitogen activated protein kinases in promoting cell wall damage and caspofungin tolerance. mBio 11:e02962-19. https://doi.org/10.1128/mBio.02962-19.

26. Winkelströter LK, Bom VL, de Castro PA, Ramalho LN, Goldman MH, Brown NA, Rajendran R, Ramage G, Bovier E, Dos Reis TF, Savoldi M, Hagiwara D, Goldman GH. 2015. High osmolarity glycerol response PtcB phosphatase is important for Aspergillus fumigatus virulence. Mol Microbiol 96:42–54. https://doi.org/10.1111/mmi.12919.

27. Valiante V, Monteiro MC, Martín J, Altwasser R, El Aouad N, González I, Kniemeyer O, Mellado E, Palomo S, de Pedro N, Pérez-Victoria I, Tormo JR, Vicente F, Reyes F, Genilloud O, Brakhage AA. 2015. Hitting the caspofungin salvage pathway of human-pathogenic fungi with the novel lasso peptide humidimycin (MDN-0010). Antimicrob Agents Chemother 59:5145–5153. https://doi.org/10.1128/AAC.00683-15.

28. Conrad T, Kniemeyer O, Henkel SG, Krüger T, Mattern DJ, Valiante V, Guthke R, Jacobsen ID, Brakhage AA, Vlaic S, Linde J. 2018. Module-detection approaches for the integration of multilevel omics data highlight the comprehensive response of Aspergillus fumigatus to caspofungin. BMC Syst Biol 12:88. https://doi.org/10.1186/s12918-018-0620-8.

29. Furukawa T, van Rhijn N, Fraczek M, Gsaller F, Davies E, Carr P, Gago S, Fortune-Grant R, Rahman S, Gilsenan JM, Houlder E, Kowalski CH, Raj S, Paul S, Cook P, Parker JE, Kelly S, Cramer RA, Latgé JP, Moye-Rowley S, Bignell E, Bowyer P, Bromley MJ. 2020. The negative cofactor 2 complex is a key regulator of drug resistance in Aspergillus fumigatus. Nat Commun 11:427. https://doi.org/10.1038/s41467-019-14191-1.

30. Blatzer M, Barker BM, Willger SD, Beckmann N, Blosser SJ, Cornish EJ, Mazurie A, Grahl N, Haas H, Cramer RA. 2011. SREBP coordinates iron and ergosterol homeostasis to mediate triazole drug and hypoxia responses in the human fungal pathogen Aspergillus fumigatus. PLoS Genet 7:e1002374. https://doi.org/10.1371/journal.pgen.1002374.

31. Amich J, Vicentefranqueira R, Leal F, Calera JA. 2010. Aspergillus fumigatus survival in alkaline and extreme zinc-limiting environments relies on the induction of a zinc homeostasis system encoded by the zrfC and aspf2 genes. Eukaryot Cell 9:424–437. https://doi.org/10.1128/EC.00348-09.

32. Denning DW. 2002. Echinocandins: a new class of antifungal. J Antimicrob Chemother 49:889–891. https://doi.org/10.1093/jac/dkf045.

33. Beauvais A, Bruneau JM, Mol PC, Buitrago MJ, Legrand R, Latgé JP. 2001. Glucan synthase complex of Aspergillus fumigatus. J Bacteriol 183:2273–2279. https://doi.org/10.1128/JB.183.7.2273-2279.2001.

34. Jaimes-Arroyo R, Lara-Rojas F, Bayram Ö, Valerius O, Braus GH, Aguirre J. 2015. The SrkA kinase is part of the SakA mitogen-activated protein kinase interactome and regulates stress responses and development in Aspergillus nidulans. Eukaryot Cell 14:495–510. https://doi.org/10.1128/EC.00277-14.

35. de Assis LJ, Manfiolli A, Mattos E, Fabri J, Malavazi I, Jacobsen ID, Brock M, Cramer RA, Thammahong A, Hagiwara D, Ries LNA, Goldman GH. 2018. Protein kinase A and high-osmolarity glycerol response pathways cooperatively control cell wall carbohydrate mobilization in Aspergillus fumigatus. mBio 9:e01952-18. https://doi.org/10.1128/mBio.01952-18.

36. Grosse C, Heinekamp T, Kniemeyer O, Gehrke A, Brakhage AA. 2008. Protein kinase A regulates growth, sporulation, and pigment formation in Aspergillus fumigatus. Appl Environ Microbiol 74:4923–4933. https://doi.org/10.1128/AEM.00470-08.

37. Fuller KK, Richie DL, Feng X, Krishnan K, Stephens TJ, Wikenheiser-Brokamp KA, Askew DS, Rhodes JC. 2011. Divergent protein kinase A isoforms co-ordinately regulate conidial germination, carbohydrate metabolism and virulence in *Aspergillus fumigatus*. Mol Microbiol 79:1045–1062. https://doi.org/10.1111/j.1365-2958.2010.07509.x.

38. Liebmann B, Mu M, Braun A, Brakhage AA. 2004. The cyclic AMP dependent protein kinase A network regulates development and virulence in *Aspergillus fumigatus*. Infect Immun 72:5193–5203. https://doi.org/10.1128/IAI.72.9.5193-5203.2004.

39. Rocha MC, Godoy KF, de Castro PA, Hori JI, Bom VL, Brown NA, Cunha AF, Goldman GH, Malavazi I. 2015. The *Aspergillus fumigatus* pkcAG579R mutant is defective in the activation of the cell wall integrity pathway but is dispensable for virulence in a neutropenic mouse infection model. PLoS One 10:e0135195. https://doi.org/10.1371/journal.pone.0135195.

40. Dichtl K, Helmschrott C, Dirr F, Wagener J. 2012. Deciphering cell wall integrity signalling in *Aspergillus fumigatus*: identification and functional characterization of cell wall stress sensors and relevant Rho GTPases. Mol Microbiol 83:506–519. https://doi.org/10.1111/j.1365-2958.2011.07946.x.

41. Irie K, Takase M, Lee KS, Levin DE, Araki H, Matsumoto K, Oshima Y. 1993. MKK1 and MKK2, which encode *Saccharomyces cerevisiae* mitogen-activated protein kinase-kinase homologs, function in the pathway mediated by protein kinase C. Mol Cell Biol 13:3076–3083. https://doi.org/10.1128/mcb.13.5.3076.

42. Lee KS, Levin DE. 1992. Dominant mutations in a gene encoding a putative protein kinase (BCK1) bypass the requirement for a *Saccharomyces cerevisiae* protein kinase C homolog. Mol Cell Biol 12:172–182. https://doi.org/10.1128/mcb.12.1.172.

43. Gustin MC, Albertyn J, Alexander M, Davenport K. 1998. MAP kinase pathways in the yeast S*accharomyces cerevisiae*. Microbiol Mol Biol Rev 62:1264–1300. https://doi.org/10.1128/MMBR.62.4.1264-1300.1998.

44. Kaneko Y, Ohno H, Imamura Y, Kohno S, Miyazaki Y. 2009. The effects of an Hsp90 inhibitor on the paradoxical effect. Jpn J Infect Dis 62:392–393.

45. Wiederhold NP, Kontoyiannis DP, Prince RA, Lewis RE. 2005. Attenuation of the activity of caspofungin at high concentrations against Candida albicans: possible role of cell wall integrity and calcineurin pathways. Antimicrob Agents Chemother 49:5146–5148. https://doi.org/10.1128/AAC.49.12.5146-5148.2005.

46. Cagas SE, Jain MR, Li H, Perlin DS. 2011. Profiling the *Aspergillus fumigatus* proteome in response to caspofungin. Antimicrob Agents Chemother 55:146–154. https://doi.org/10.1128/AAC.00884-10.

47. Bradford MM. 1976. A rapid and sensitive method for the quantitation of microgram quantities of protein utilizing the principle of protein-dye binding. Anal Biochem 72:248–254. https://doi.org/10.1006/abio.1976.9999.

48. Larsen MR, Thingholm TE, Jensen ON, Roepstorff P, Jørgensen TJ. 2005. Highly selective enrichment of phosphorylated peptides from peptide mixtures using titanium dioxide microcolumns. Mol Cell Proteomics 4:873–886. https://doi.org/10.1074/mcp.T500007-MCP200.

49. Palmisano G, Parker BL, Engholm-Keller K, Lendal SE, Kulej K, Schulz M, Schwämmle V, Graham ME, Saxtorph H, Cordwell SJ, Larsen MR. 2012. A novel method for the simultaneous enrichment, identification, and quantification of phosphopeptides and sialylated glycopeptides applied to a temporal profile of mouse brain development. Mol Cell Proteomics 11:1191–1202. https://doi.org/10.1074/mcp.M112.017509.